CONF-9509182--2
SAND95-0008C

Computational Analysis of a Three-Dimensional High-Velocity Oxygen-Fuel (HVOF) Thermal Spray Torch*

Basil Hassan, Amalia R. Lopez, and William L. Oberkampf

Sandia National Laboratories

Albuquerque, New Mexico

Abstract

An analysis of a High-Velocity Oxygen-Fuel Thermal Spray torch is presented using computational fluid dynamics (CFD). Three-dimensional CFD results are presented for a curved aircap used for coating interior surfaces such as engine cylinder bores. The device analyzed is similar to the Metco Diamond Jet Rotating Wire torch, but wire feed is not simulated. To the authors' knowledge, these are the first published 3-D results of a thermal spray device. The feed gases are injected through an axisymmetric nozzle into the curved aircap. Argon is injected through the center of the nozzle. Premixed propylene and oxygen are introduced from an annulus in the nozzle, while cooling air is injected between the nozzle and the interior wall of the aircap. The combustion process is modeled assuming instantaneous chemistry. A standard, two-equation, k-ε turbulence model is employed for the turbulent flow field. An implicit, iterative, finite volume numerical technique is used to solve the coupled conservation of mass, momentum, and energy equations for the gas in a sequential manner. Flow fields inside and outside the aircap are presented and discussed.

HIGH-VELOCITY OXYGEN-FUEL (HVOF) THERMAL SPRAYING employs a combustion process to heat the gas flow and coating material. The two-phase gas and particle flow is then accelerated to high velocities. The combustion process produces temperatures in the range of 3000 K inside the thermal spray device which result in supersonic streams exterior to the device. In contrast, plasma spray devices typically attain temperatures in the range of 10,000 K where significant ionization of the carrier gas can occur. These high temperatures typically produce lower density, subsonic flows with lower velocities as compared to HVOF.

Advances in computational fluid dynamics (CFD) have made their way into thermal spray modeling. Modern CFD incorporates detailed modeling of such physical phenomena as turbulence, chemical reactions, and multi-phase flows so as to provide an in-depth understanding of the spray process and aid in torch design.

CFD simulations have been done in two-dimensions, primarily on axisymmetric thermal spray devices both with and without powder injection. The first CFD simulation of the HVOF process was conducted by Power et. al.[1,2] and Smith et. al.[3]They modeled the internal and external flow of the Metco Diamond Jet torch with a powder feeder. Since the flow was choked at the exit of the nozzle, the internal flow was solved separately from the external flow. A two-step finite-rate chemistry model was used to model the combustion of propylene (C_3H_6). For the external flow, it was assumed that all the propylene is combusted inside the nozzle and that the oxidation of carbon monoxide is small. They assumed that the flow at the exit of the nozzle was fully mixed and had reached chemical equilibrium. Therefore, the external flow computations were performed without chemical kinetics and only mixing with the ambient air was modeled. Particles of various sizes were injected inside the aircap and tracked subject to the local gas velocity and temperature. However, the effects of the particles on the gas stream were not modeled.

Oberkampf and Talpallikar[4,5] also analyzed the fluid and particle dynamics of a similar axisymmetric geometry. The combustion of propylene was modeled by a one-equation, approximate equilibrium chemistry model that accounts for dissociation of the combustion products. Their work considered full coupling between the interior and exterior flow fields. In addition, the numerical algorithm used an Eulerian/Langrangian approach for the gas and solid phases. The two phases are fully coupled through momentum and energy exchanges that appear as source terms in the governing equations. Their approach allowed for particle temperatures and velocities that were different than that of the local gas flow. Finally, they investigated such characteristics as trajectories and phase state of the sprayed powder.

The current work will present CFD calculations made on a three-dimensional aircap similar to the Metco Diamond Jet Rotating Wire torch. A solid model representation of this aircap is shown in Fig. 1. The work will concentrate on the gas dynamic aspects of these com-

* This work was performed at Sandia National Laboratories, which is operated by Lockheed Martin for the U. S. Department of Energy under Contract DE-AC04-94AL85000.

MASTER

DISTRIBUTION OF THIS DOCUMENT IS UNLIMITED

DISCLAIMER

This report was prepared as an account of work sponsored by an agency of the United States Government. Neither the United States Government nor any agency thereof, nor any of their employees, makes any warranty, express or implied, or assumes any legal liability or responsibility for the accuracy, completeness, or usefulness of any information, apparatus, product, or process disclosed, or represents that its use would not infringe privately owned rights. Reference herein to any specific commercial product, process, or service by trade name, trademark, manufacturer, or otherwise does not necessarily constitute or imply its endorsement, recommendation, or favoring by the United States Government or any agency thereof. The views and opinions of authors expressed herein do not necessarily state or reflect those of the United States Government or any agency thereof.

DISCLAIMER

Portions of this document may be illegible in electronic image products. Images are produced from the best available original document.

plex, three-dimensional flow fields. Features of both the interior and exterior flow fields including temperature, Mach number distributions, and streamline patterns are presented and discussed.

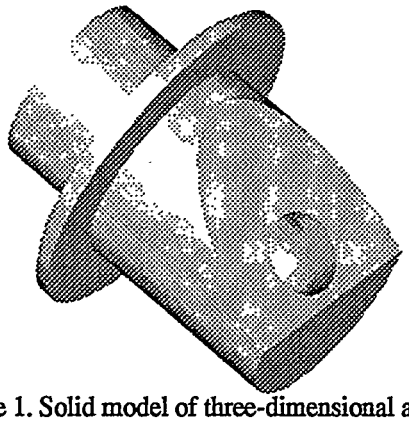

Figure 1. Solid model of three-dimensional aircap.

Gas Dynamics Modeling

The numerical simulations are made using a commercial CFD code, CFD-ACE.[6,7] CFD-ACE is a pressure-based code that solves the three-dimensional, Favre-averaged Navier-Stokes equations which are a statement of conservation of mass, momentum, and energy for unsteady, compressible, turbulent flows. The governing equations are solved sequentially in an implicit, iterative manner using a finite volume formulation. The code includes various options for modeling turbulence, reaction chemistry, and multi-phase flows. For the present calculations, the governing equations are solved until a steady-state result is achieved. In addition, the k-ε turbulence model of Launder and Spaulding[8] is used along with the compressibility correction of Sarkar.[9] For further details on the numerical algorithm, see Refs. 6-7.

Chemistry Modeling

Modeling of hydrocarbon chemistry can take many forms of varying complexity. The number of intermediate species and reactions that can occur in hydrocarbon-air reaction models is typically large. Efforts at using reduced finite-rate reactions have shown mixed results, depending on how the rate coefficients are derived. Given that the time scales associated with the chemistry are much shorter than that at which the fluid convects, the assumption of equilibrium chemistry can be made. Oberkampf and Talpallikar[4,5] reported that the typical Gibbs free energy minimization technique for computing full equilibrium chemistry can be computationally intensive and produce numerical instabilities near the inlets of the premixed streams.

Their approach made use of an approximate, instantaneous equilibrium technique. This same approach is used in the CFD calculations that are presented in this paper. A one-step reaction was derived from the One-Dimensional Equilibrium Chemistry code developed by Gordon and McBride[10] and is of the form:

$$C_3H_6 + x\,O_2 \Rightarrow Products$$

where x is the number of moles of oxygen that react with one mole of propylene. The products of combustion in their analysis included CO_2, H_2O, CO, H_2, OH, H, and, O. Argon (Ar), the carrier gas, and nitrogen (N_2) were assumed inert at the temperatures considered. Inputting a specified fuel/oxygen mixture ratio, pressure, and temperature (those of the premixed fuel and oxygen stream), the One-Dimensional Equilibrium Chemistry code[10] determines the equilibrium composition and from this the following balanced reaction can be defined:

$$C_3H_6 + 3.552\,O_2 \Rightarrow 1.036\,CO_2 + 1.964\,CO + 1.937\,H_2O + 0.733\,OH + 0.476\,H_2 + 0.441\,H + 0.398\,O$$

The above reaction will go to completion at every point in the flow field, regardless of the local temperature and pressure.

Aircap Geometry and Grid Generation

The geometry to be studied is similar to a Metco Diamond Jet Rotating Wire torch. A schematic of the interior of the curved aircap is shown in Fig. 2. The interior is composed of a converging conical section and two cylindrical sections blended together by a portion of a sphere. The turn angle between the centerlines of the two cylinders is 60 degrees. There are three sets of inlet streams: the argon center stream, the premixed fuel and oxygen stream, and the air cooling stream along the surface of the aircap. In the Metco hardware, the fuel/oxygen stream is fed by ten equally spaced holes around the circumference of the nozzle. For computational purposes, the fuel/oxygen inlet is simplified as an annulus that has the same total area as the ten holes and is centered at the same radial location as the holes in the nozzle.

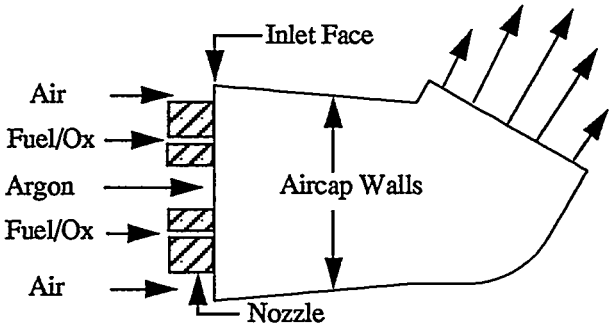

Figure 2. Schematic of the interior of the three-dimensional HVOF Thermal Spray torch.

The centerline of the nozzle (i.e., argon and fuel/oxygen inlets) has been shifted vertically upward, i.e., the y-direction, by 0.406 mm (0.016 in.) from the centerline of the conical portion of the aircap. This shift provides

more air cooling flow to the bottom portion of the aircap where the heat transfer rates will be higher, primarily in the curved region of the aircap near the exit. Both the premixed fuel/oxygen and the air cooling streams enter the aircap at an angle of 5 degrees, which is the half angle of the conical section.

The inner radius of the aircap at the inlet face of the torch is 5.59 mm (0.22 in.) and the outer radius of the nozzle is 4.13 mm (0.1625 in.). The outer radius of the fuel/oxygen annulus is 3.10 mm (0.1222 in.) and the inner radius is 2.79 mm (0.1098 in.). The radius of the argon inlet is 1.91 mm (0.075 in.). Finally, the aircap exit radius is 4.41 mm (0.1735 in.).

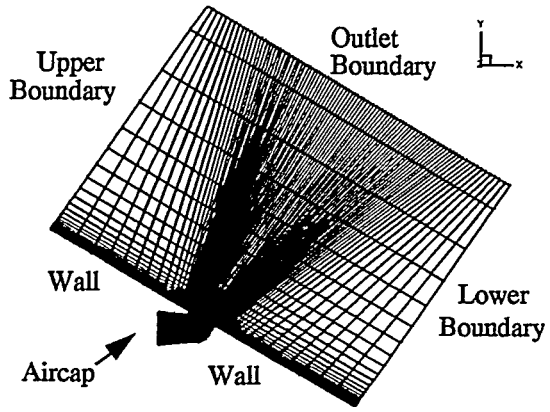

Figure 3. Interior and exterior grid in plane of symmetry (every other grid line shown).

The computational grid used in the CFD calculations was created using GRIDGEN Version 10.[11] The computational grid in the plane of symmetry is shown in Fig. 3, along with the exterior boundaries. (The solid black region of the grid is due to very dense grid clustering of the grid cells.) The grid was created in two blocks: the interior of the aircap and the exterior where the jet decay occurs. The upper and lower boundaries extend 13 aircap exit radii from the centerline and the outlet boundary extends 20 aircap exit radii from the aircap exit. It was only necessary to solve half the domain due to symmetry about the *x-y* plane.

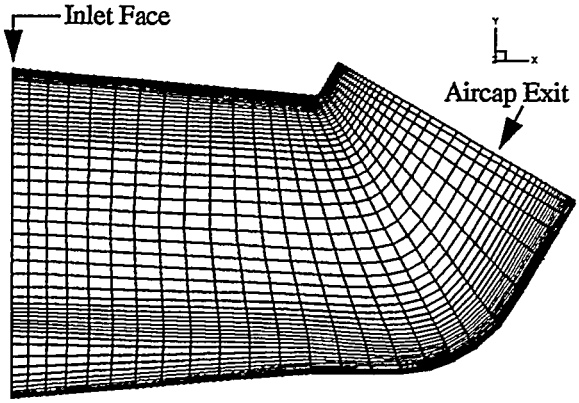

Figure 4. Interior aircap grid in plane of symmetry (every other grid line shown).

The computational domain in the aircap begins at the inlet where the argon, fuel/oxygen, and air streams enter the aircap. The plane of symmetry grid in the interior of the aircap is shown in Fig. 4. Radial grid clustering was performed in the regions of the shear layers surrounding the fuel/oxygen inlets and in the boundary layer on the surface of the aircap. In addition, grid cells were clustered in the jet decay region outside the torch. The grid cell dimensions are 50 (axial) x 50 (radial) x 18 (circumferential) in the interior and 50 (axial) x 92 (radial) x 18 (circumferential) in the exterior region. The total number of grid cells in the three-dimensional calculation domain was 127,800. These results were only computed on a single grid and future work will address grid convergence.

Boundary Conditions

Mass flow rates and gas temperatures are specified at all three inlets and are listed in Table 1. All walls are modeled with a no-slip, fixed temperature condition. The wall temperature on the nozzle, i.e., between the three inlet streams was 320 *K*. The specified wall temperature of the aircap increased linearly with *x* from 310 *K* at the inlet to 420 *K* at the aircap exit. The value at the exit was determined experimentally. It was felt that the linear variation in temperature would be more accurate than specifying a constant temperature over the entire aircap surface. For a more accurate prediction of aircap wall temperature, a coupled fluid/solid heat conduction calculation, which can be more computationally intensive, must be performed.

The HVOF torch is assumed to exhaust into ambient air at a temperature of 303 K and a sea-level pressure of 101,325 Pa (1 atm). In the exterior block, the boundary surrounding the aircap exit is a fixed temperature, no-slip wall, the upper and lower outer boundary is a fixed pressure inlet/outlet, and the outlet boundary makes use of an extrapolation boundary condition. The plane of symmetry uses a symmetry condition in both the interior and exterior blocks.

Table 1 Mass Flow Rates and Inlet Temperatures

Gas	Mass Flow Rates		Temperature
	SCFH	*kg/sec*	*K*
Argon	20.0	2.572×10^{-4}	310.0
Propylene	100.0	1.350×10^{-3}	320.0
Oxygen	450.0	4.630×10^{-3}	320.0
Air	1100.0	1.024×10^{-2}	310.0

Computational Requirements

The computational simulations were initially converged with a first-order upwind spatial discretization scheme for 1500 iterations. Since first-order upwind can be very numerically dissipative and artificially smear out high gradient regions in the flow, the solution was

restarted with a mixed second-order, central difference/ upwind scheme and run for 1500 more iterations. The solution required 4.49 *msec/cell/iteration* of CPU time and 129 *Mbytes* of RAM on a Sun Microsystems SPARCstation 10 Model 51 workstation. These 3000 iterations required a total CPU time of 478 hours.

Results

Internal Flow Field. The gas temperature contours in the plane of symmetry of the aircap are shown in Fig. 5. The premixed fuel and oxygen enter the aircap in an annular stream and instantaneously react to form the products of combustion considered in the model. Recirculating flow regions exist on either side of the fuel/oxygen inlet and act as a flame holder. The peak temperature in the flow field is 3150 K, and this value is consistent with calculations made using the One Dimensional Equilibrium Chemistry code of Gordon and McBride.[10] The combustion region is confined on the outside by the cold air entering along the surface of the aircap. The air cooling is required to maintain acceptable levels of heat transfer to the aircap surface. The air cooling layer on the bottom of the aircap is thicker due to the vertical shift between the torch and the aircap, which is necessary to keep the curved portion of the aircap from melting and/or eroding. The centerline offset technique works very effectively in keeping the bottom portion of the aircap cooler, while minimally increasing the heating to the upper aircap wall.

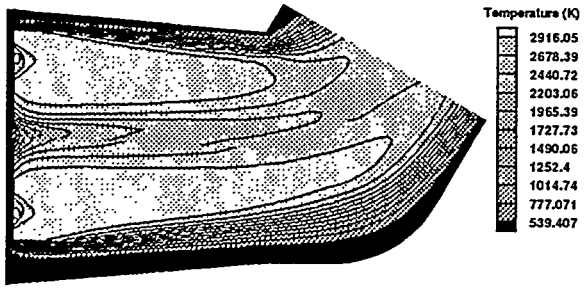

Figure 5. Plane of symmetry gas temperature contours inside aircap.

Instantaneous chemistry assumes that the time scale of the reaction is much smaller than that of the convective fluid, or infinitely fast rates. Though it produces the correct levels of peak temperatures in the flow field, it does not allow for any ignition delay. A finite-rate reaction model, on the other hand, would enable the gradual ignition over a finite distance and more accurately represent the combustion process. Current work is being conducted to investigate finite-rate chemistry models for hydrocarbon combustion in order to have improved predictions.

Figure 6 shows the streamline patterns in the plane of symmetry of the aircap. On the upper surface of the aircap, near the exit, the boundary layer separates from the wall as the flow tries to turn the sharp corner. It can be observed in the streamline plot that flow from the ambient region is actually sucked into the aircap above the separated region.The main ignition zone is seen by the highly curved streamlines near the fuel/oxygen inlet.

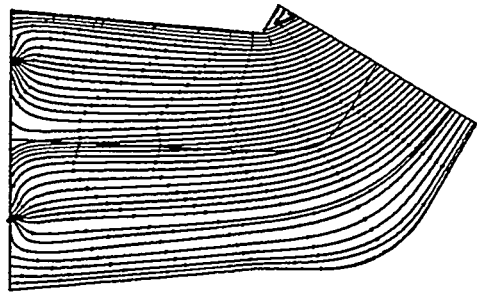

Figure 6. Plane of symmetry streamline patterns inside aircap.

Figure 7 shows gas Mach number contours in the circular exit plane of the aircap, i.e., normal to the view in previous figures. The inflow region discussed in the previous figure is seen to extend over a significant portion near the top of the aircap exit. The sharp corner near the exit at the top of the aircap, which caused the separated shear layer, transitions into a smooth, spherical shape at the bottom of the aircap as one moves around the circumference. As the geometry becomes smoother and the effective turn angle decreases, the shear layer diffuses and ultimately disappears. One can also observe in Fig. 7 that the region below the shear layer is only partially supersonic at the exit. This means that the sonic surface is distorted in shape and lies both inside and outside the exit of the aircap. The distortion of the sonic surface near the exit occurs due to the non-uniform flow field of the mixing streams and the large variation in static temperature in the streams as seen in Fig. 5.

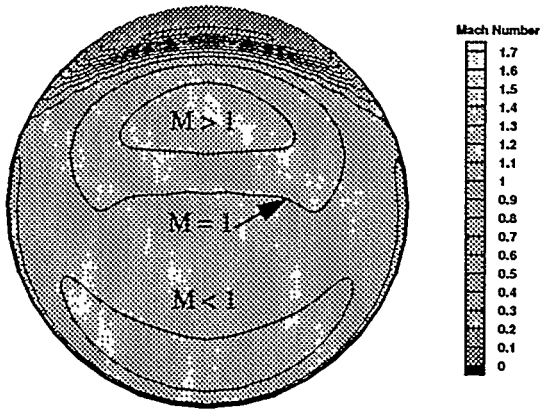

Figure 7. Gas Mach number contours in the exit plane of the aircap.

External Flow Field. Gas Mach number contours in the plane of symmetry are shown in Fig. 8. For the mass flow rates given, there is sufficient energy from combustion to choke the flow near the exit of the aircap. In Fig. 8, the nonuniform Mach number distribution near the exit can clearly be seen. The peak Mach number in the supersonic jet occurs about one exit radius from the aircap and has a value of 1.7. Recall that the Mach num-

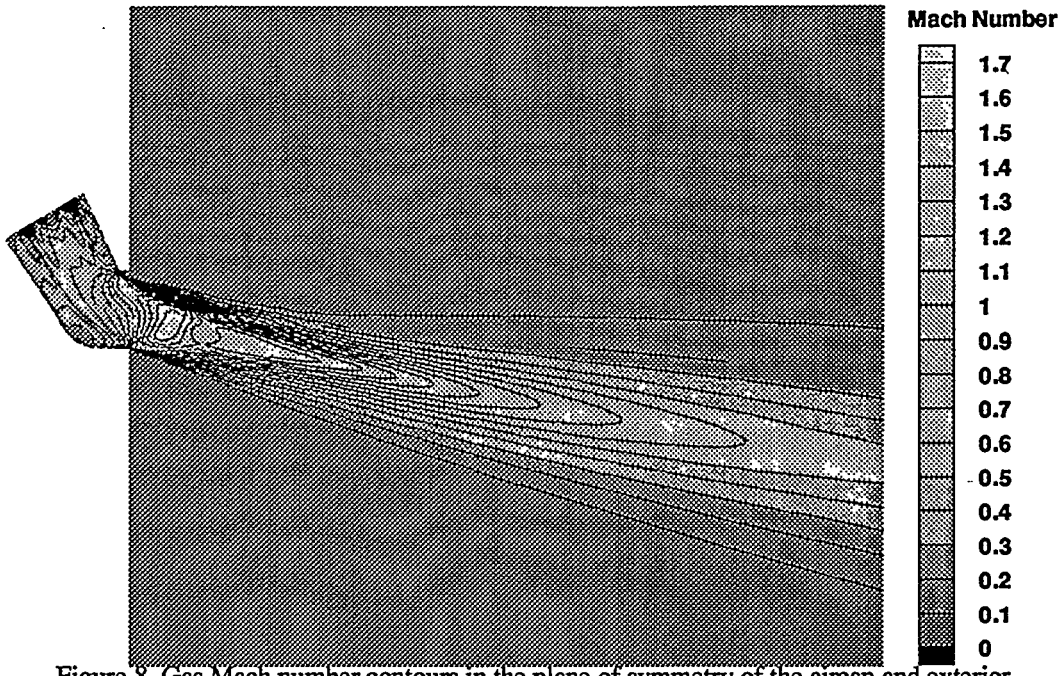

Figure 8. Gas Mach number contours in the plane of symmetry of the aircap and exterior.

ber is the ratio of the local gas speed to the local speed of sound. Because of the high gas temperatures in the jet, the local speed of sound at the peak Mach number is about 1200 m/sec.

Since the pressure exiting the aircap is higher than the ambient pressure, this underexpanded jet will then supersonically expand to the ambient pressure through a series of expansion and compression waves, known as shock diamonds. Two distinct shock diamonds can be seen in the flow field. The strength of the expansion and compression waves decreases as the flow convects downstream and the supersonic core flow is dissipated due to mixing with the ambient air. The supersonic region only extends approximately halfway through the exterior portion of the calculation domain.

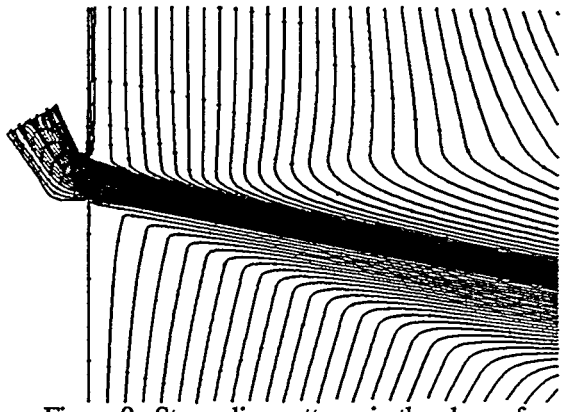
Figure 9. Streamline patterns in the plane of symmetry of the aircap and exterior.

Streamline patterns in the plane of symmetry are shown in Fig. 9. It can clearly be seen that the jet angle is not as large as the geometric turn angle of the aircap. The jet has been directed downward by the separated shear layer that exists on the upper portion of the aircap near the exit. The predicted spray angle of the torch for these operating conditions is approximately 50 degrees, whereas the geometric turn angle is 60 degrees. As the jet exhausts into the ambient air, a "pumping" effect results as the ambient air is entrained into the high speed jet. Inflow from the top and bottom boundaries occurs due to the entrainment. The peak velocity in the jet is about 1500 *m/sec* and decreases to a value of 300 *m/sec* at the exit of the computational domain.

Not only does the jet velocity decrease away from the aircap, but so does the gas temperature of the jet as seen in Fig. 10. The cold ambient air mixes with the hot jet and cools the flow as it convects downstream. The gas temperature is approximately 2500K at the aircap exit. The temperature drops in the first expansion wave to about 2200 K, approximately 6 mm downstream of the exit. Next, the temperature rises in the first compression to about 2350 K, approximately 10 mm downstream. Finally, the temperature decreases to about 900 K at the exit of the computational domain. High temperature, low density jets of this type will tend to decrease in temperature much faster than cold jets due to the rapid mixing that takes place with the cold ambient air.

Summary and Future Work

Computational solutions for a geometry similar to a Metco Diamond Jet Rotating Wire torch have been presented for both the internal combusting flow and external jet decay. Gas temperature, Mach number distributions, and streamline patterns were discussed to illustrate the features of this complex three-dimensional flow. The peak temperature in the combustor was 3150 K, and the peak Mach number in the jet was 1.7. The

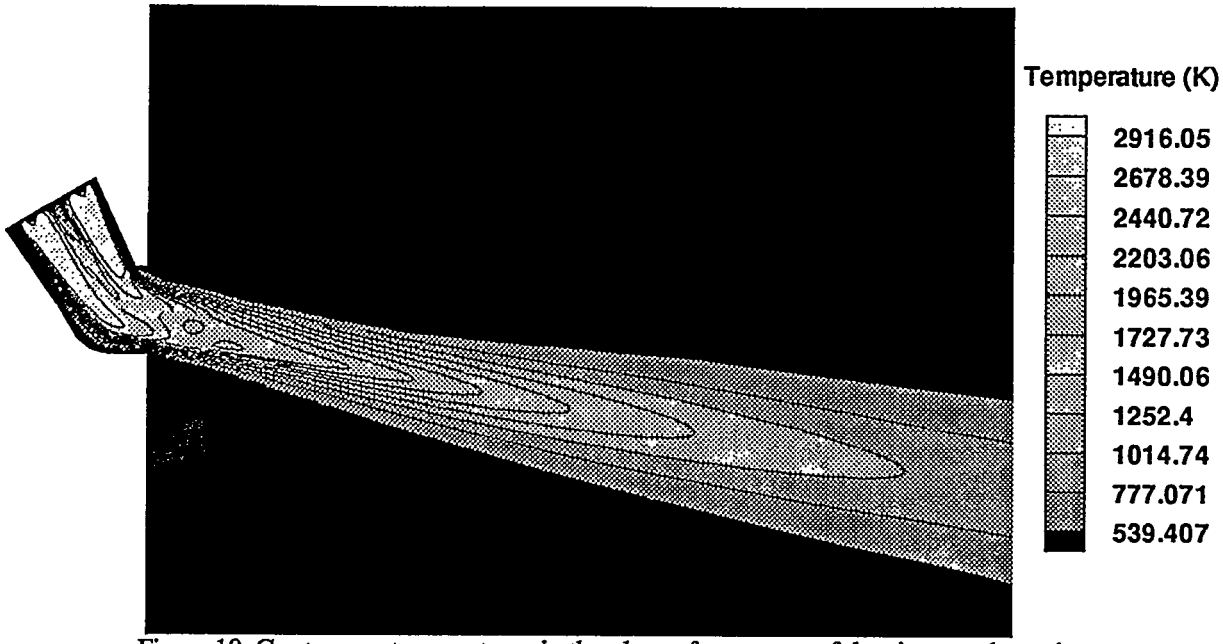

Figure 10. Gas temperature contours in the plane of symmetry of the aircap and exterior.

predicted spray angle of the jet was seen to be ten degrees less than the geometric turn angle of the aircap. This paper represents the first published computational solutions of a three-dimensional thermal spray torch. Details of the flow features determined through CFD calculations that cannot normally be measured experimentally should be useful in the design of future aircaps.

Future work will investigate coupling of spray particle dynamics and heat transfer with the gas dynamics for these three-dimensional flows. In addition, a finite-rate chemistry model will be developed and implemented to better simulate the combustion process inside the aircap. The predictions will also be compared to future experimental aircap pressure and particle velocity measurements in order to validate and build confidence in the numerical technique for computing thermal spray flows.

Acknowledgements

The authors wish to thank Fritz Owens and Lyle Johnson of CFD Research Corporation for their assistance throughout this investigation.

This work was supported under United States Department of Energy, Cooperative Research and Development Agreement No. SC92-01104.

References

[1] Power, G. D., Barber, T. J., and Chiappetta, L. M., "Analysis of High Velocity Oxygen Fuel (HVOF) Thermal Torch," AIAA Paper No. 92-3598, July 1992.

[2] Power, G. D., Smith, E. B., Barber, T. J., and Chiappetta, L. M., "Analysis of a Combustion (HVOF) Spray Deposition Gun," UTRC Report 91-8, East Hartford, CT, March 1991.

[3] Smith, E. B., Power, G. D., Barber, T. J., and Chiappetta, L. M.,"Application of Computational Fluid Dynamics to the HVOF Thermal Spray Gun," Proceedings of the International Thermal Spray Conference, Orlando, FL, May, 1992, pp. 805-810.

[4] Oberkampf, W. L., and Talpallikar, M., "Analysis of a High-Velocity Oxygen-Fuel (HVOF) Thermal Spray Torch, Part 1: Numerical Formulation," Proceedings of the 7th National Thermal Spray Conference, Boston, MA, June, 1994, pp. 381-386.

[5] Oberkampf, W. L., and Talpallikar, M., "Analysis of a High-Velocity Oxygen-Fuel (HVOF) Thermal Spray Torch, Part 2: Computational Results," Proceedings of the 7th National Thermal Spray Conference, Boston, MA, June, 1994, pp. 387-392.

[6] Lai, Y. G., Przekwas, A. J., and So, R. M. C., "Aerodynamic Flow Simulation Using a Pressure-Based Method and a Two-Equation Turbulence Model," AIAA Paper No. 93-2902, July 1993.

[7] Jiang, Y., Lai, Y. G., Ho, S. Y., and Przekwas, A. J., "3D Simulations of Complex Flows with an Implicit Multi-Domain Approach," AIAA Paper No. 93-3124, July 1993.

[8] Launder, B. E., and Spaulding, D. B., "The Numerical Calculation of Turbulent Flows," *Computational Methods Applied to Mechanics and Engineering*, Vol. 3, 1974, pp. 269-289.

[9] Sarkar, S., "The Analysis and Modeling of Dilatational Terms in Compressible Turbulence," Journal of Fluid Mechanics, Vol. 227, 1991, PP. 473-493.

[10] Gordon, S., and McBride, B. J., "Computer Program for Calculation of Complex Chemical Equilibrium Compositions, Rocket Performance, Incident and Reflected Shocks, and Chapman-Jouguet Detonations," NASA SP-273, Interim Revision, March 1976, (New Version 1989).

[11] GRIDGEN User's Manual, Version 10, Pointwise, Inc., Bedford, TX, March 1995.